Supplementary Information (SI) for Journal of Materials Chemistry A.
This journal is © The Royal Society of Chemistry 2025

Experimental Section

Electrolyte Synthesis: $PbSnF_4$ was synthesized by the following steps: The following reagents were the starting compounds for synthesis: high-purity Pb $(NO_3)_2$ (99.99%, Aladdin); analytically pure NH_4F (99.99%, Aladdin), SnF_2 (99.99%, Aladdin), LiF (99.99%, Aladdin). Firstly, a solution of Pb $(NO_3)_2$ in distilled water was gradually added a threefold excess of a NH_4F solution, the product is obtained through precipitation. Afterward, washing the resulting precipitate several times with distilled water, then dried at 353 K for about 5 h and calcined the γ-PbF_2 at 753-773 K with a heating rate of 5℃ min^{-1}. "As a result, β-PbF_2 was obtained as a precursor. Subsequently, PbF_2 and LiF were thoroughly ground, mixed in a 1:3 molar ratio, and pressed into pellets. The resulting pressed mixtures were heated to 873 K with a heating rate of 5℃ min^{-1} to obtain the final sintered $PbSnF_4$ in quartz tubes in a high-purity argon atmosphere and held at this temperature for 5 h with subsequent cooling to room temperature with switched-off furnace. In the third stage, the obtained solid solutions were fused with equimolar amounts of SnF_2 in crucibles in an argon atmosphere, held at 773 K with a heating rate of 5 ℃ min^{-1} for 20 min and cooled to room temperature with switched-off furnace. After all the steps, the obtained were nonstoichiometric $PbSnF_4$@LiF phases. At last, stoichiometric amounts of the materials were mixed in the agate mortar, and then milled using WC balls (5 mm diameter) and WC jars (45 ml) on a planetary mill; the milling was conducted at 500 rpm for 8 h in Ar atmosphere, and the ball-to-powder ratio was 20:1. It was important that all steps should be completed under argon protection.

Composite Electrode Material Preparation: because of the reason that CuF_2 has a poor F^- ionic conductivity and electron conductivity, engineering of an additional ionic and electronic were required in order to prepared the composite cathode of CuF_2-$PbSnF_4$@LiF-C (abbreviated as CPC). From this point of views, the conductive carbon and the solid electrolyte $PbSnF_4$@LiF were mixed into cathode in order to increase the ionic and electronic conductors in CPC cathode. A typical high-energy ball milling procedure (with a rotating speed of 600 rpm for 5 h) was implemented for the mixture of commercial anhydrous CuF_2 (99.99%, Aladdin), as-prepared $PbSnF_4$@LiF and Super P with a mass ratio of 3:6:1.

In view of the poor F^- ionic conductivity and less reactive interfaces of pure metal anodes, the additional ionic wiring engineering was required to prepare the composite anode of Pb+PbF_2- $PbSnF_4$@LiF -C (abbreviated as PPC). This composite anode was prepared by mixing Sn (99.9%, Aladdin), SnF2, KSn2F5, and Super P with a mass ratio of 2.5:2.5:4:1 using the typical high-energy ball milling procedure (with a rotating speed of 600 rpm for 5 h).

Ionic and Electronic Conduction Estimation of $PbSnF_4$@LiF: putting 120mg $PbSnF_4$@LiF inside the metal mold, then pressed it into a pellet with a diameter of 10mm under the pressure of 200 MPa for 2 minutes. Then the construction of ionic blocking layer was executed via blading conductive gold paste on both sides of the pellet, followed by drying at 80 °C for 2 h. Note that, the drying step should be completed under argon protection. Subsequently, Au | $PbSnF_4$@LiF | Au was assembled into a button cell in order to measure impedance performance though an

electrochemical workstation with a frequency range from 10 MHz to 100 Hz and an excitation voltage of 100 mV. Ionic conductivity can be estimated by equation (3):

$$\sigma = \frac{L}{RS} \tag{3}$$

where L, S, and R denote the thickness, area, and resistance of the pellet, respectively.

Preparation of Electrodes: The cathode was prepared by mixing CPC powder, binder poly (vinyl difluoride) (PVDF, Sigma-Aldrich, dissolved in 1-methyl-2-pyrrolidinone, Sinopharm Chemical Reagent Co., Ltd, ≧99.0%, with a mass concentration of 1 mg per 20 μL) and conductive carbon (Super P, MTI Corporation) with a weight ratio of 7:1:2. The slurry anode was prepared by mixing PPC powder, PVDF, and conductive carbon with a weight ratio of 7:1:2. Then both the cathode and anode slurries were pasted on the pure Al and Cu foils, and then dried at the temperature of 60 °C for 12 h in vacuum.

Fabrication and Operation of ASSFIBs: for the better integration of solid -solid interfaces, the THF solution with 1 m TBAF(Aladdin) was used as the interface wetting regent because the reason that its relative stability and ideal F^- conductivity. In the progress during battery assembling, the both sides of the pressured pellet would be dropped about 3 μL TBAF/THF solution to get wet. Then the anode and cathode membranes (both Φ10) were appressed to each side of the electrolyte pellet surface. LSV test was based on the full cells using above technique. The measurement of electrochemical window of the $PbSnF_4$@LiF electrolyte would be test in architecture of Pb+PbF_2|$PbSnF_4$@LiF|$PbSnF_4$@LiF-C cell was also conducted on this

electrochemical workstation at a scan rate of 1.0 mV s^{-1}. The as-assembled Pb+PbF_2 | $PbSnF_4$@LiF | CuF_2 cell was placed into an oven at 80 °C for 5 h with the follow-up galvanostatic discharge–charge cycling performance measurement on the Land multichannel battery testing system (CT2001A) at the same temperature. The galvanostatic discharge–charge tests were carried out at a current density of 60 mA g^{-1} with a discharge cut-off voltage of −0.4 V (versus Pb/PbF_2) and a charge cut-off specific capacity of 300 mAh g^{-1}.

Characterization of Materials: The crystal structure and phase purity of the synthesized materials were studied by powder X-ray diffraction (XRD) using Cu Kα1 radiation in a 2θ range from 10° to 80° at a scanning rate of 10° min^{-1} to detect the evolution of chemical composition, elemental valence, and bonding situation of the material at different post-reaction states. The samples were sealed using parafilm during measurement to prevent air exposure. The SEM observation was conducted using a SEM (Nova NanoSEM450) scanning electron microscope operated at 3 kV. And the nanostructure of the solid electrolyte interphase (SEI) was examined using transmission electron microscopy (TEM). Note that, for all the ex-situ characterizations, the post-reaction samples were drawn out from the disassembled batteries and then sealed in a bottle in the Ar-filled glove box before the transfer to the corresponding testing chamber.

Supporting figures:

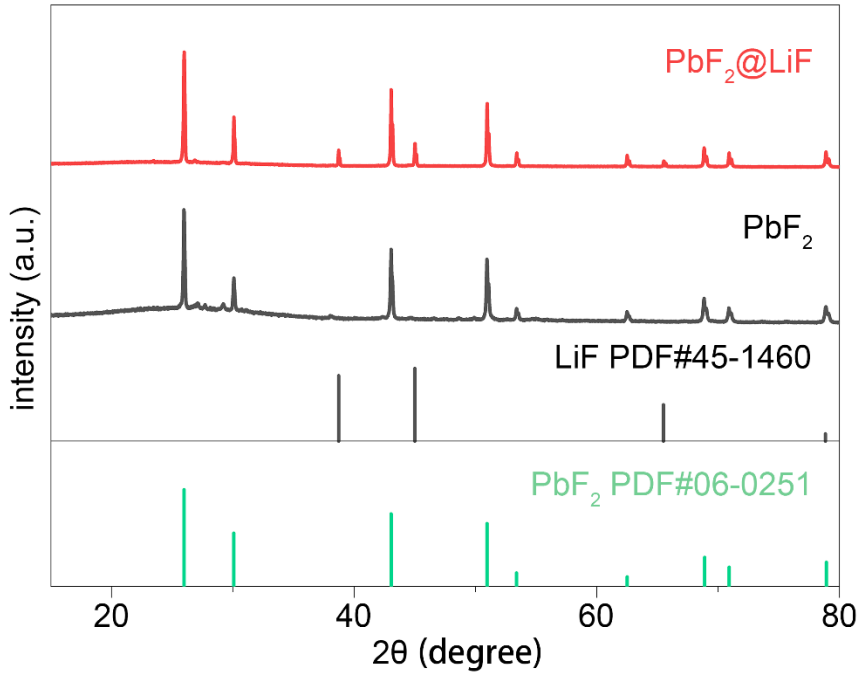

Figure S1. XRD patterns of PbF_2 and PbF_2@LiF.

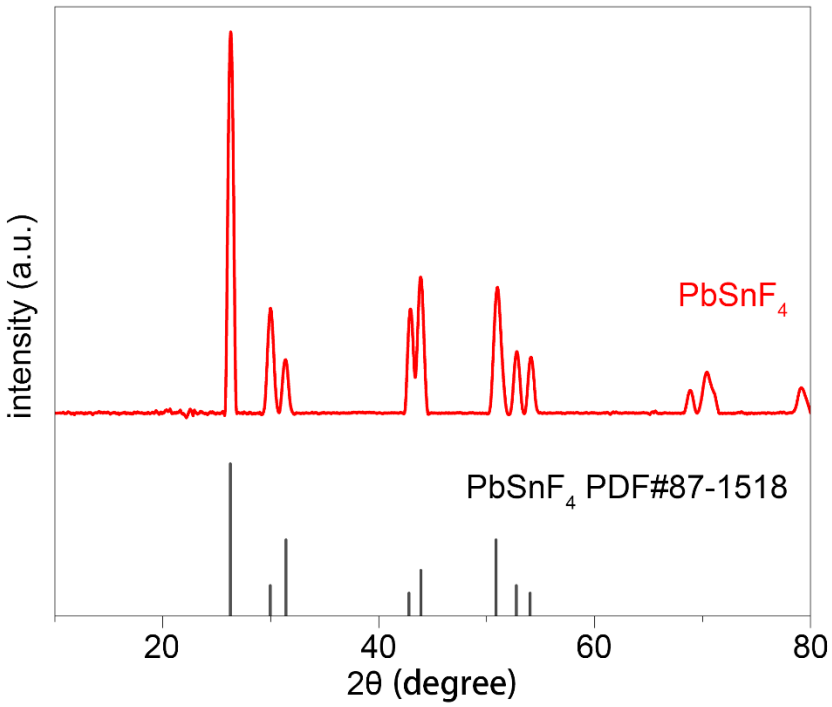

Figure S2. XRD pattern of synthetic $PbSnF_4$.

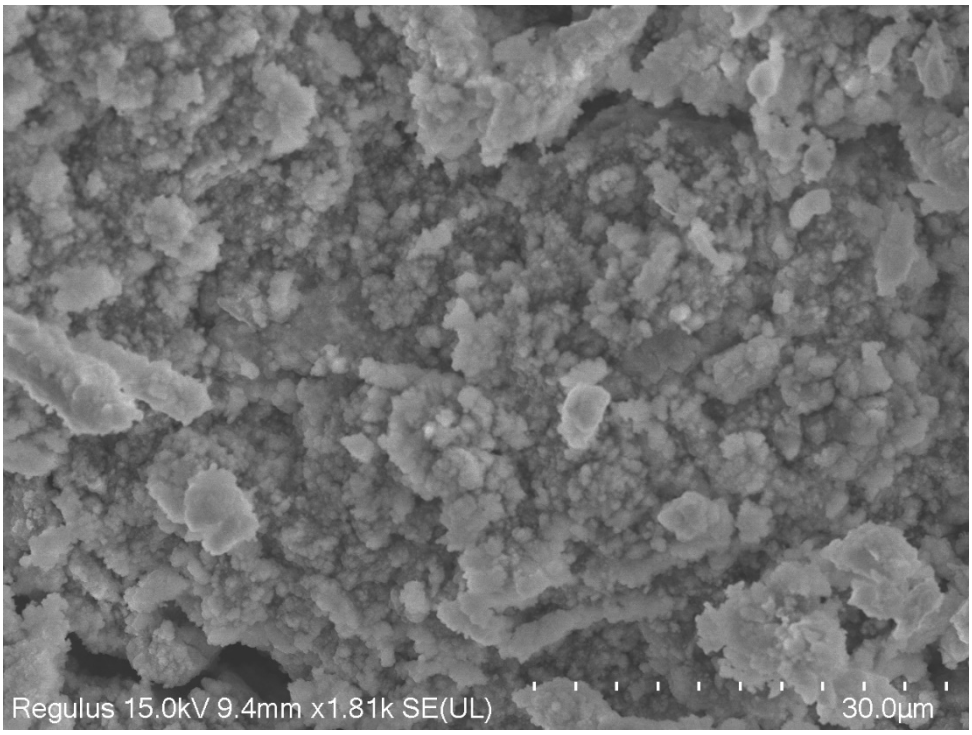

Figure S3. SEM image of the morphology of $PbSnF_4$ powders.

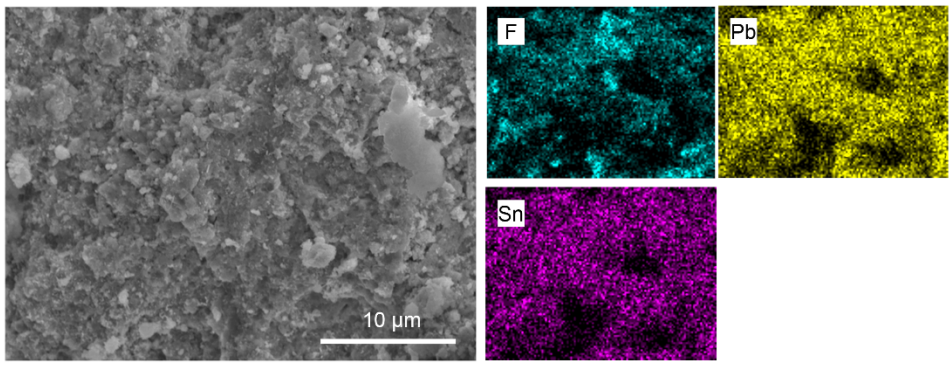

Figure S4. SEM image and the corresponding EDS mapping results of the $PbSnF_4$ powders.

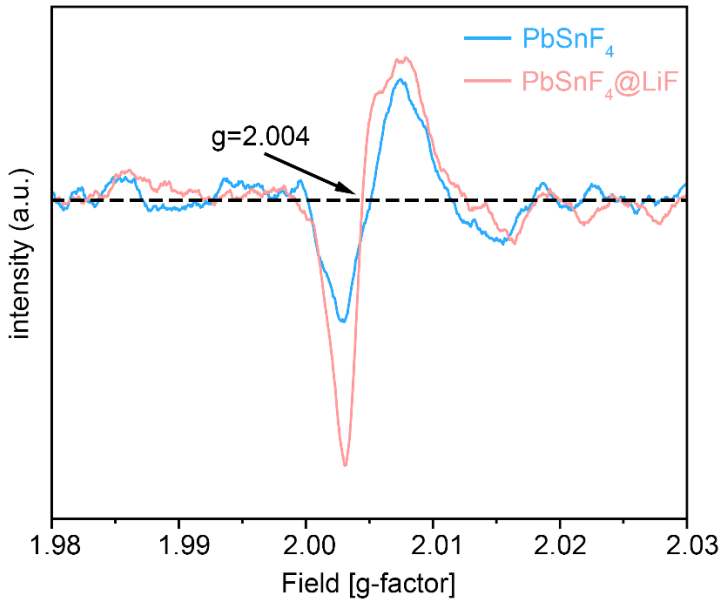

Figure S5. EPR testing of fluorine vacancies in $PbSnF_4$ and $PbSnF_4$@LiF.

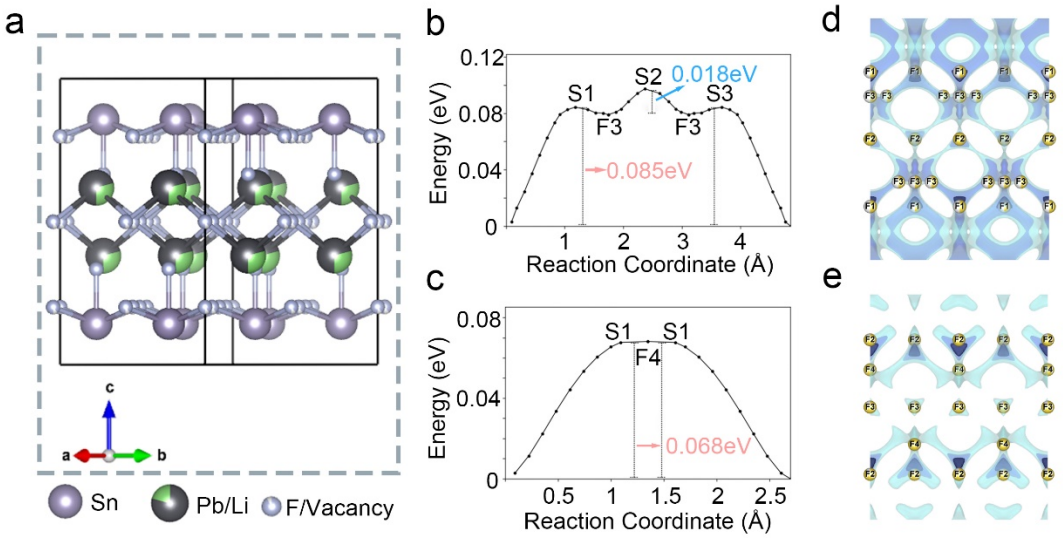

Figure S6. (a) The crystal structure of $PbSnF_4$@LiF unit cell was visualized using VESTA. (b) The migration barrier energy of F-ions through different sites in $PbSnF_4$@LiF and $PbSnF_4$. (d and e) Schematic diagram of fluoride ion transport pathways in $PbSnF_4$@LiF and $PbSnF_4$.

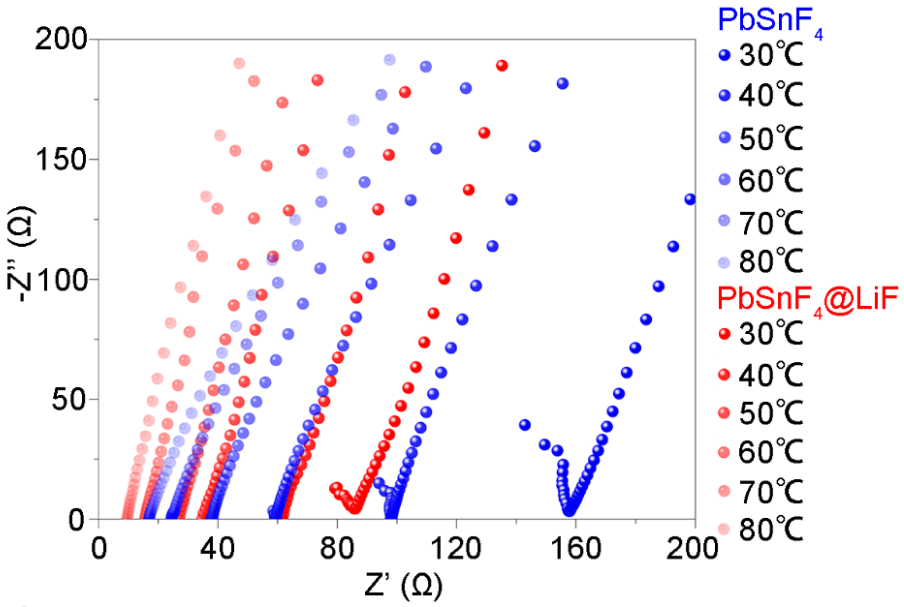

Figure S7. Nyquist plots of $PbSnF_4$ and $PbSnF_4$@LiF at different temperatures (30-80 ℃).

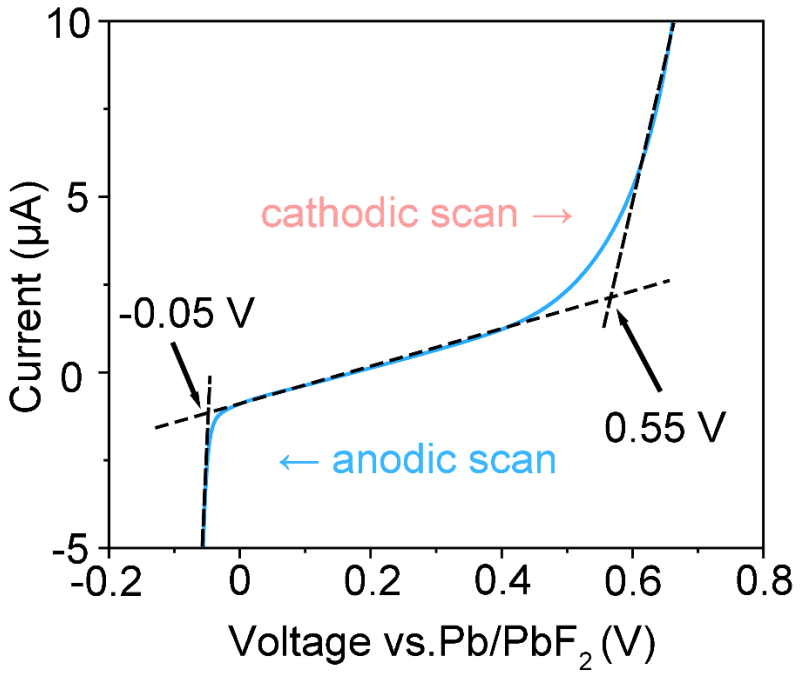

Figure S8. LSV curves of the CuF_2|$PbSnF_4$ |Pb+PbF_2 full cell at 0.02 mV s^{-1}.

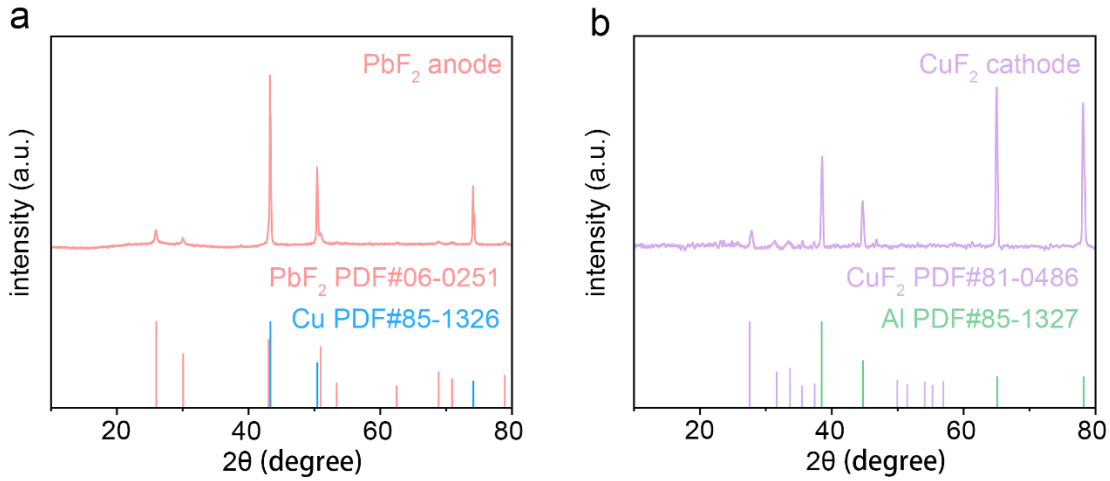

Figure S9. XRD patterns of the synthesized (a) PbF_2 anode and (b) CuF_2 cathode materials.

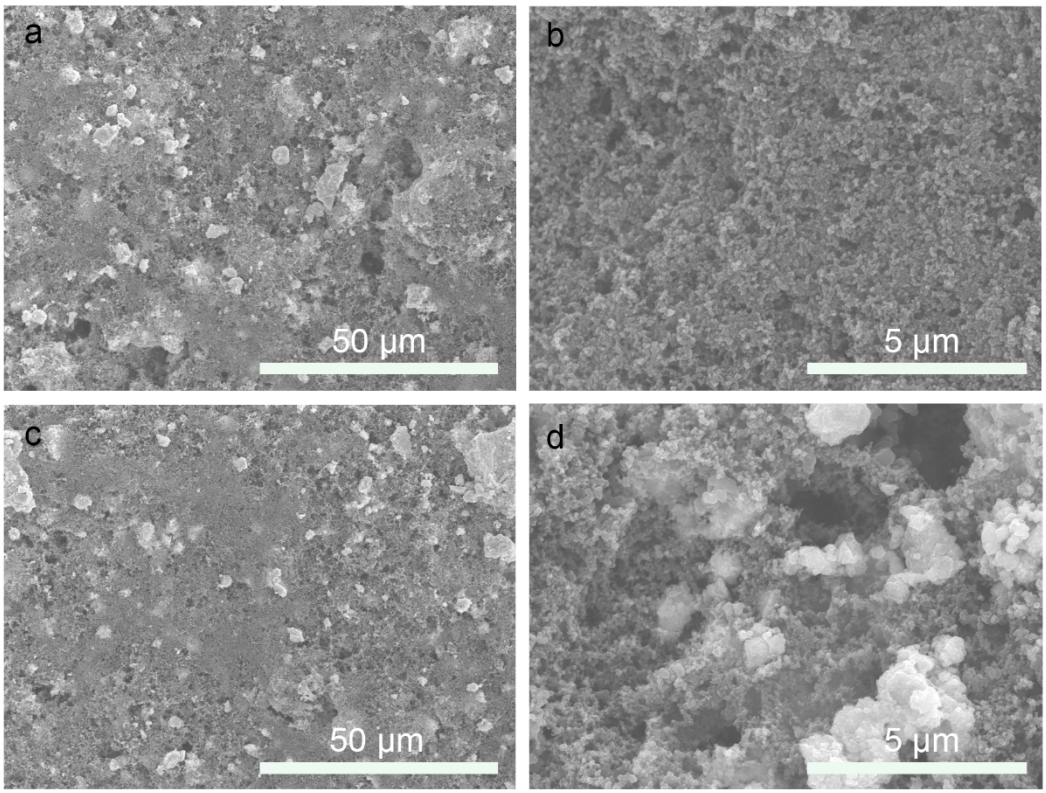

Figure S10. SEM images of the synthesized PbF_2 anode (a and b) before cycling and (c and d) after 10 cycles.

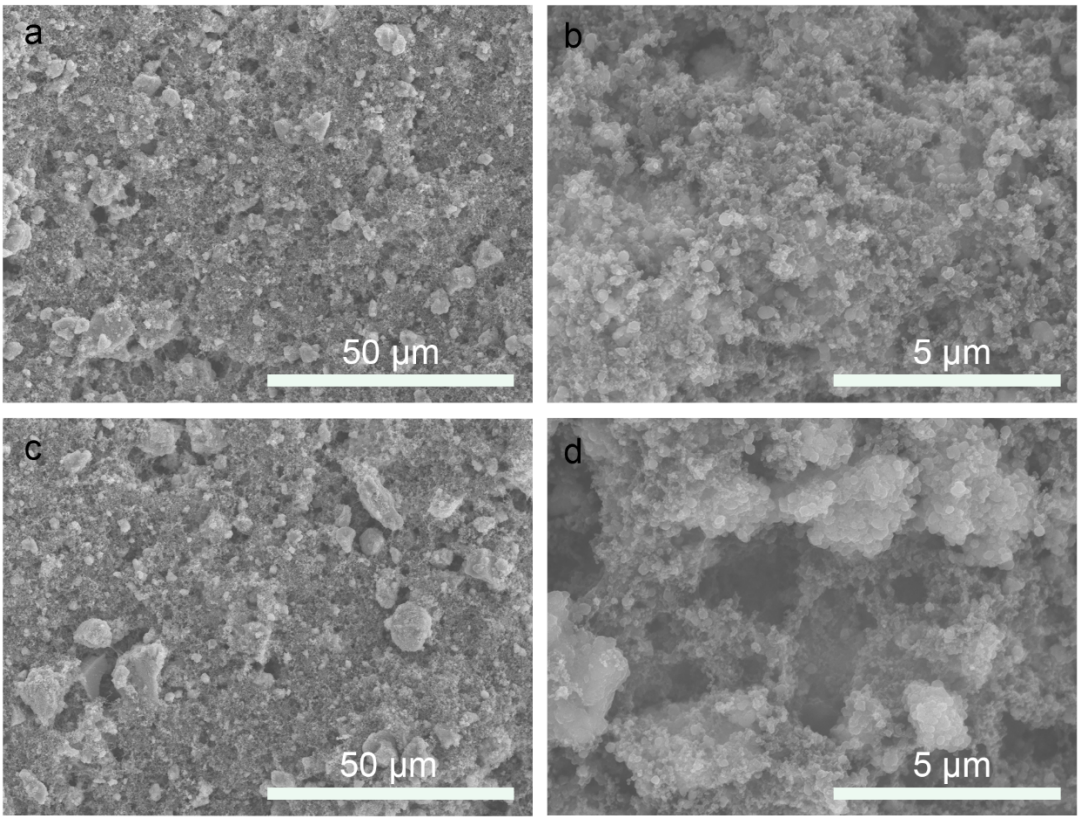

Figure S11. SEM patterns of the synthesized CuF_2 cathode (a and b) before cycling and (c and d) after 10 cycles.

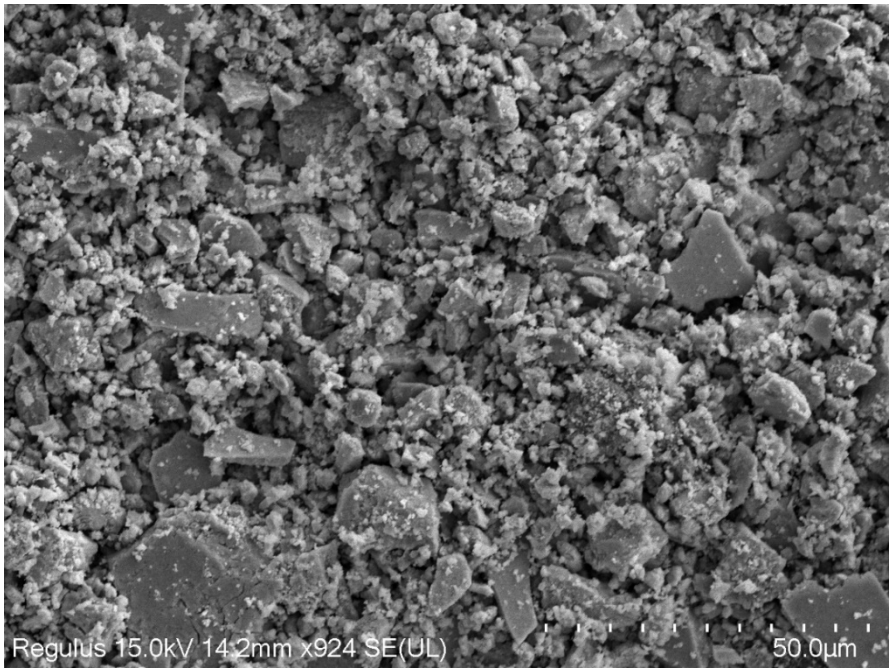

Figure S12. SEM image of the morphology of CuF_2 cathode.

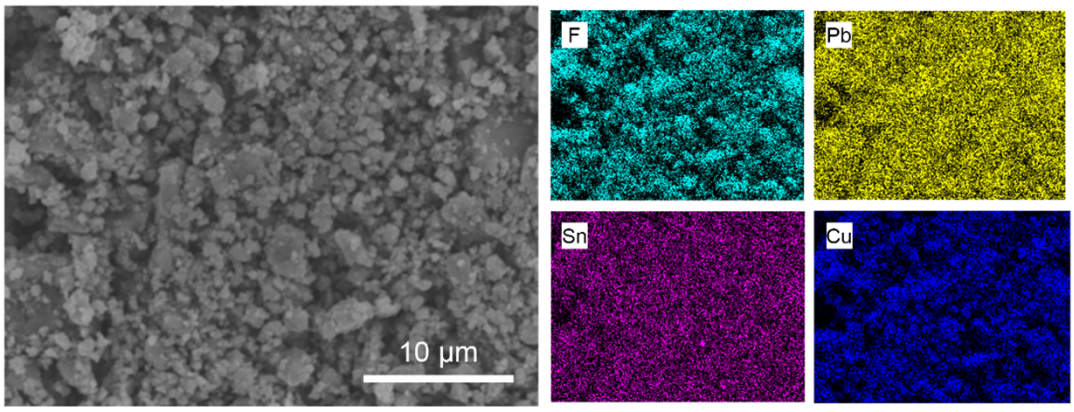

Figure S13. SEM image and the corresponding EDS mapping results of the CuF_2 cathode.

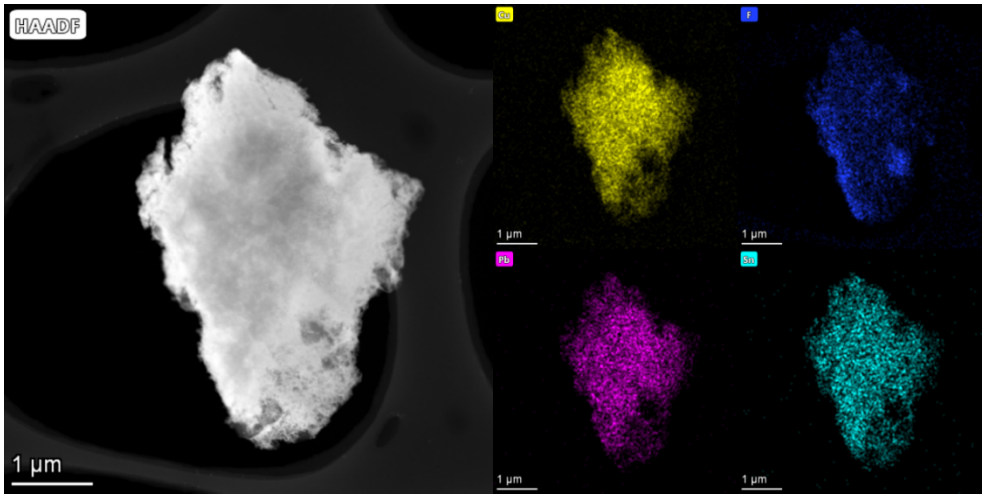

Figure S14. STEM image and the corresponding EDS mapping results of the CuF_2 cathode.

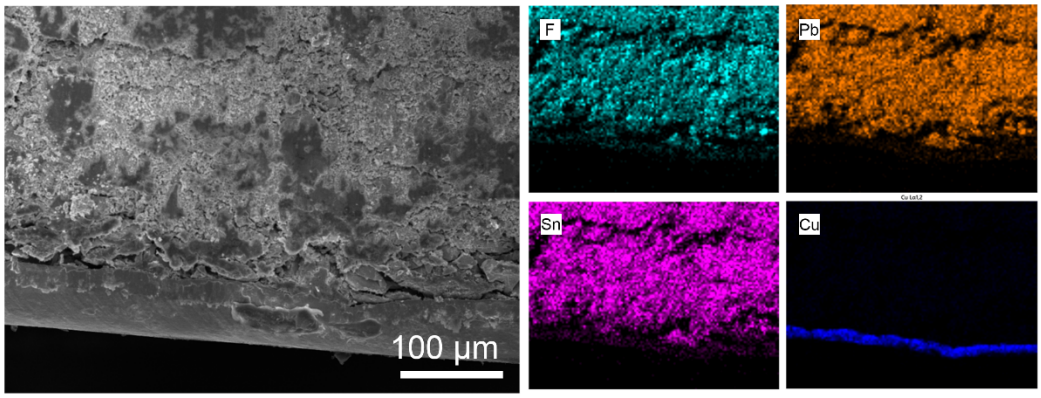

Figure S15. SEM image and the corresponding EDS mapping results of the CuF_2 cathode after cycling.

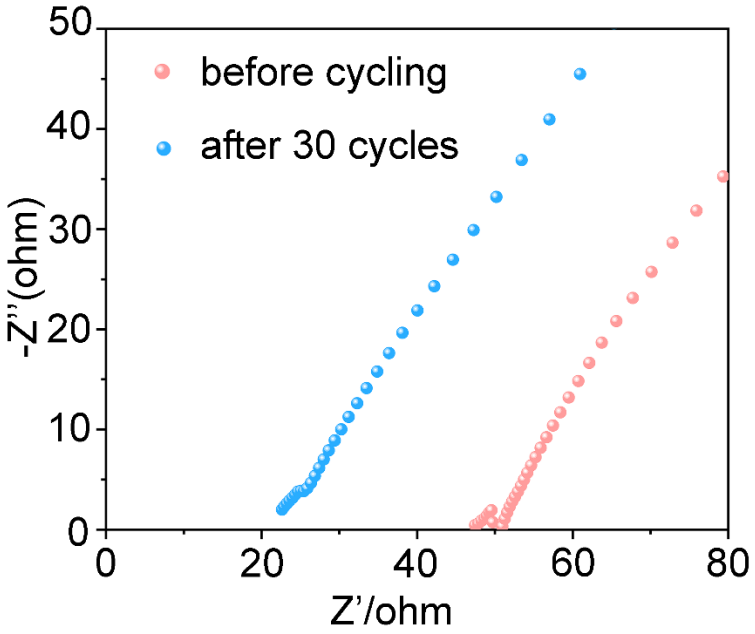

Figure S16. EIS patterns of CuF_2|$PbSnF_4$@LiF|Pb+PbF_2 full cells before cycling and after 30 cycles.

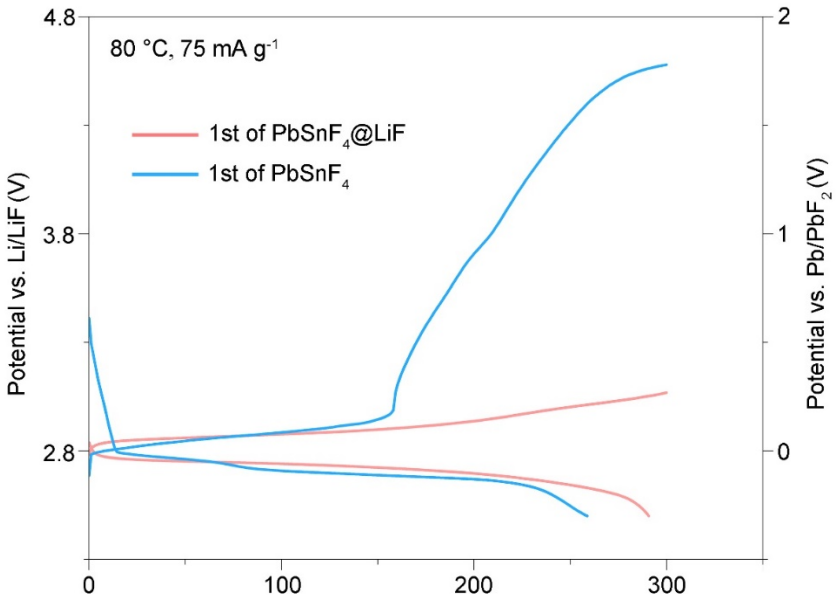

Figure S17. The initial discharge/charge curves of the assembled $CuF_2|PbSnF_4|Pb+PbF_2$ and $CuF_2|PbSnF_4@LiF|Pb+PbF_2$ full cells at the current density of 75 mA g^{-1} with a capacity of 300 mAh g^{-1}.

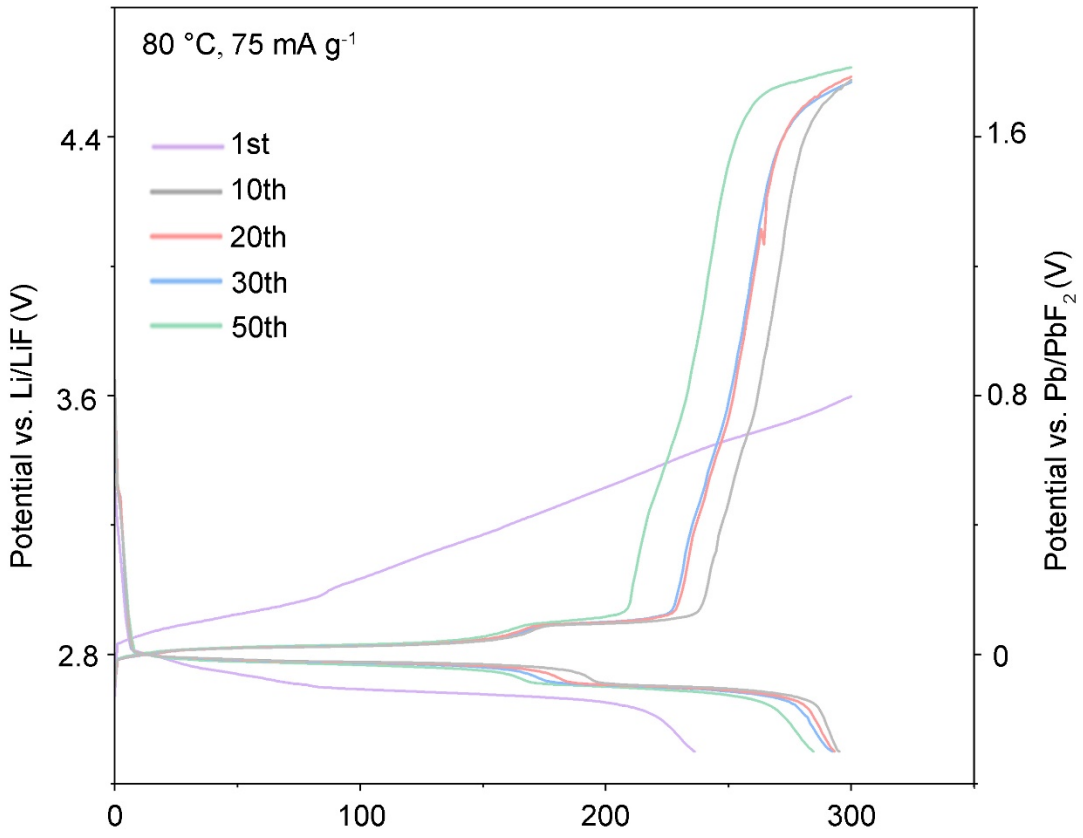

Figure S18. The discharge/charge curves of the $CuF_2|PbSnF_4|Pb+PbF_2$ full cell after 1-50 cycles at the current density of 75 mA g^{-1}.

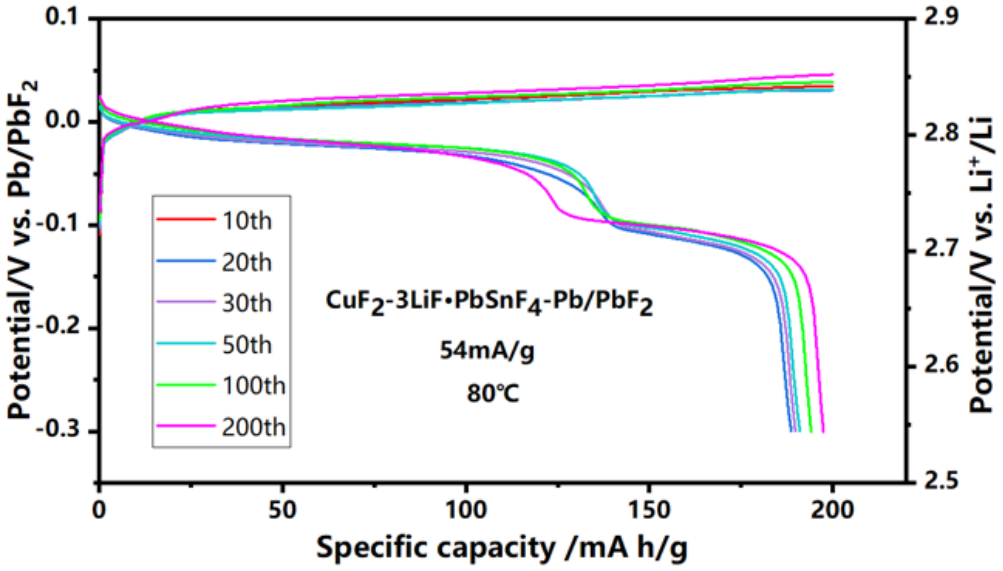

Figure S19. The voltage-capacity curves of the assembled CuF_2|3LiF-$PbSnF_4$|Pb/PbF_2 full cells at room temperature with a capacity of 200 mAh g^{-1}.

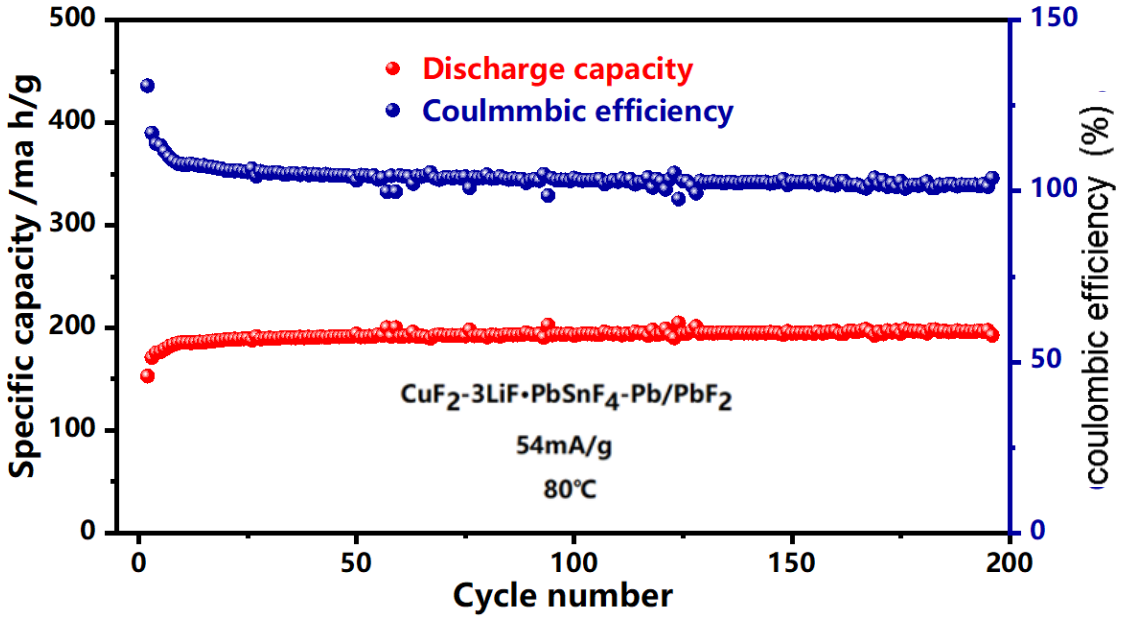

Figure S20. The cycling performance of the $CuF_2|3LiF{\cdot}PbSnF_4|Pb/PbF_2$ full cell with a capacity of 200 mAh g^{-1}.

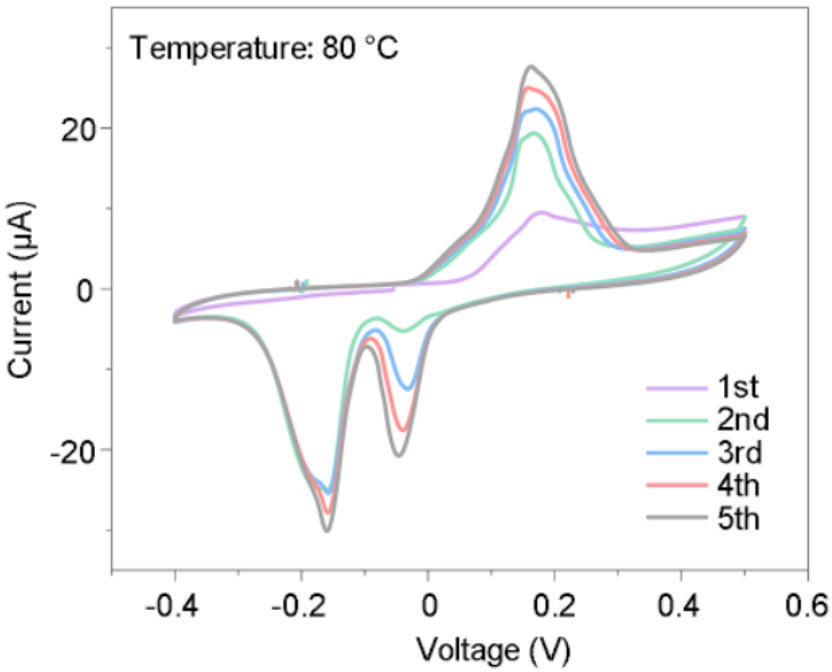

Figure S21. CV curves of the CuF_2|$PbSnF_4$@LiF|Pb+PbF_2 full cell at 0.02 mV s^{-1}.

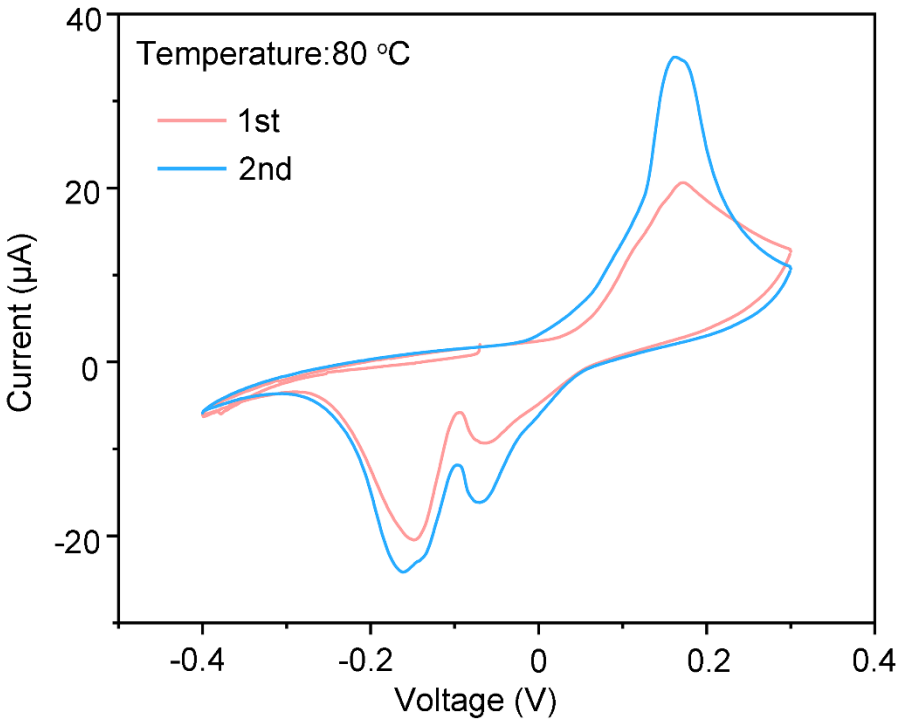

Figure S22. CV curves of the CuF_2|$PbSnF_4$ |Pb+PbF_2 full cell at 0.02 mV s^{-1}

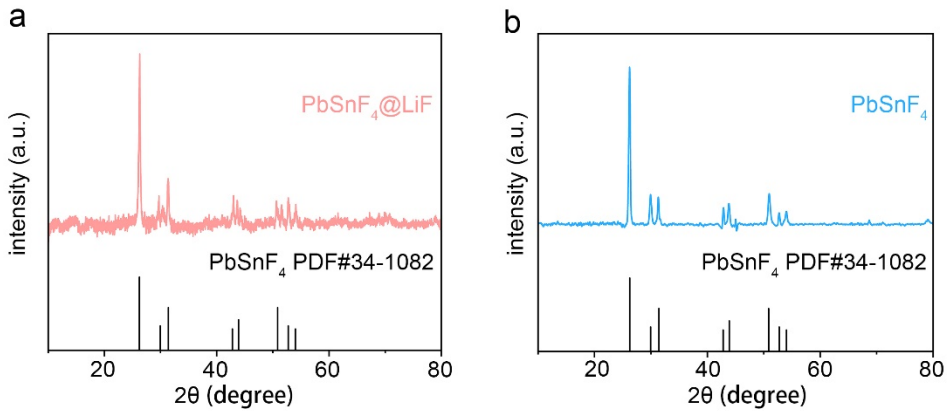

Figure S23. XRD patterns of the obtained (a) $PbSnF_4$@LiF and (b) $PbSnF_4$ after cycles.

Table S1. Summary of the performance of all solid-state fluoride ion batteries assembled with various solid electrolytes.

Cathode/SE/Anode	Cycle number	Current density (mA g^{-1})	Tempe -rature (℃)	Capacity at 1_{st} discharge (mAh g^{-1})	Capacity Retention (mAh g^{-1})
BiF_3/ $PbSnF_4$/Sn	120	40	25	115.6	102.1
BiF_3/ $PbSnF_4$/Sn	100	8	-20	90.1	84.6
$Sr_3Fe_2O_5F_2$/$La_{0.9}Ba_{0.1}F_{2.9}$/Pb-PbF_2	70	5	140	94.4	118
CuF_2/ $La_{0.95}Sr_{0.05}F_{2.95}$/Pb-$PbF_2$	10	9.5	25	410	459
GLG300/ $La_{0.97}Ba_{0.03}F_{2.97}$	9	0.63	75	155	144
Ag/SSR-PK10/ Pb-PbF_2	100	6	25	190.6	152
CuF_2/ KSn_2F_5/Sn-SnF_2	70	20	60	442.7	150
BiF_3/ $PbSnF_4$/ Pb-PbF_2	50	10	25	210.5	173.9
BiF_3/ $PbSnF_4$/Sn	10	10	25	175	80
BiF_3/$Ba_{0.95}Ce_{0.05}SnF_{4.05}$/Sn	30	10	25	170.9	84.5
BiF_3/$La_{0.95}Ba_{0.05}F_{2.95}$/Ce	8	4	60	245	90
CuF_2/$La_{0.9}Ba_{0.1}F_{2.9}$/La	23	4	150	360	40
BiF_3/$Ba_{0.98}Eu_{0.02}F_{4.02}$/Sn	20	10	25	106	72
BiF_3/ $La_{0.9}Ba_{0.1}F_{2.9}$-$BaSnF_4$/Ce	5	10	150	251	119

Table S2. Structure parameters of β-$PbSnF_4$.

Atom	site	x	y	z	Occupancy
Sn	2c	0	0.5	0.142840	1
Pb	2c	0	0.5	0.618920	0.7
Li	2c	0	0.5	0.618920	0.3
F	2c	0	0.5	0.334240	1
F	4f	0	0	0.201400	0.9
F	2b	0	0	0.500000	0.9

The space group is P4/nmm. Refined lattice parameters are a = 4.3685 Å, b = 4.3685 Å, c = 11.0854 Å.